Check for updates

View Article Online
View Journal

Catalysis Science & Technology

Accepted Manuscript

This article can be cited before page numbers have been issued, to do this please use: S. Sasidharan, N. Watanabe, G. M. Anilkumar, B. N. Nair, G.S. Sailaja, T. Tamaki and T. Yamaguchi, *Catal. Sci. Technol.*, 2019, DOI: 10.1039/C8CY02232A.

This is an Accepted Manuscript, which has been through the Royal Society of Chemistry peer review process and has been accepted for publication.

Accepted Manuscripts are published online shortly after acceptance, before technical editing, formatting and proof reading. Using this free service, authors can make their results available to the community, in citable form, before we publish the edited article. We will replace this Accepted Manuscript with the edited and formatted Advance Article as soon as it is available.

You can find more information about Accepted Manuscripts in the author guidelines.

Please note that technical editing may introduce minor changes to the text and/or graphics, which may alter content. The journal's standard Terms & Conditions and the ethical guidelines, outlined in our author and reviewer resource centre, still apply. In no event shall the Royal Society of Chemistry be held responsible for any errors or omissions in this Accepted Manuscript or any consequences arising from the use of any information it contains.

ROYAL SOCIETY OF CHEMISTRY

rsc.li/catalysis

View Article Online
DOI: 10.1039/C8CY02232A

Electro-oxidation Competency of Palladium Nanocatalysts over Ceria-Carbon Composite Support during Alkaline Ethylene Glycol Oxidation

Sasidharan Sankar [†,‡], Naoto Watanabe [†], Gopinathan M. Anilkumar [§,‡], Balagopal N. Nair [§], Sailaja G. Sivakamiammal [±], Takanori Tamaki [†,‡], Takeo Yamaguchi [†,‡*]

[†] *Laboratory for Chemistry and Life Sciences, Tokyo Institute of Technology, R1-17, 4259 Nagatsuta, Midori-ku, Yokohama 226-850*
**E-mail: yamag@res.titech.ac.jp*

[‡] *Core Research for Evolutionary Science and Technology, Japan Science and Technology Agency (JST-CREST), Japan 102-0076*

[§] *R&D Centre, Noritake Co., Ltd., 300 Higashiyama, Miyochi-cho, Miyoshi, Japan 470-0293*

[±] *Cochin University of Science and Technology, Kochi, India 682022*

Published on 17 December 2018. Downloaded on 12/18/2018 12:59:19 AM.

Catalysis Science & Technology Accepted Manuscript

ABSTRACT

Direct alcohol fuel cells (DAFCs) are widely regarded as one of the most promising among the futuristic and capable energy systems; the direct liquid fuel cells (DLFCs). In this article, we discuss in detail, the competency of palladium nanoparticles developed over carbon-ceria composite supports (Pd/C-CeO_2) as efficient and durable anode catalyst for the alkaline electrooxidation of ethylene glycol (EGOR). For the first time, a systematic assessment on the EGOR performance of palladium catalysts with varying Pd-Ceria ratio is been reported. The scalable solid–solution route reduction technique enabled the processing of Pd nanoparticles with controlled morphology, size and excellent CeO_2 interaction. The structural features of the prepared catalysts were studied using x-ray diffraction, electron microscopy (TEM) and x-ray photon spectroscopy techniques, while the electrochemical performance of the catalysts were analyzed using cyclic voltammetry and chronoamperometry. During alkaline EGOR, the Pd/C-CeO_2 catalysts showed an enhanced current density (as high as **68.5 mAcm^{-2}**), more negative onset potential, excellent mass activity (**4.6 Amg$^{-1}_{Pd}$**) and exceptional durability compared to Pd/C. The enhanced alkaline EGOR kinetics for the Pd/C-CeO_2 catalysts is well attributed to the promotion effect of CeO_2 on Pd by creating more Pd-OH_{ads} and also improved tolerance to poisoning species on the Pd surface. Further, the enhanced ECSA for Pd/C-CeO_2 also has aided the excellent EGOR in alkaline medium. The validated enhanced oxidation ability of these Pd/C-CeO_2 catalysts for the anodic oxidation of other low molecular weight alcohol fuels including methanol and ethanol showcased the possible application potential toward DMFCs and DEFCs.

Key Words: Alkaline Fuel Cell, DAFC, Anode Catalyst, Palladium-Ceria, Ethylene Glycol Oxidation

View Article Online
DOI: 10.1039/C8CY02232A

Published on 17 December 2018. Downloaded on 12/18/2018 12:59:19 AM.

1. Introduction

Direct liquid fuel cells (DLFCs) have been increasingly sought after owing to their distinct advantages over other fuel cell counterparts such as polymer electrolyte membrane fuel cells (PEMFCs).[1] DLFCs are considered as revolutionary candidates of electric power production for vehicles, residential applications, high tech portable devices etc. Though proton exchange membrane based fuel cells (PEM FCs) are more widely studied, their widespread commercialization is limited due to requirement of gaseous hydrogen as fuel. The various problems associated with the use of hydrogen, such as safety, storage, and absence of distribution infrastructure have limited the rapid full scale adaptation of PEMFC technology.[2] Under these circumstances, low molecular weight alcohol liquids such as ethylene glycol, ethanol, methanol etc., which offers the prospects of easy handling and storage as well as high energy density are considered to be appropriate alternatives.[3-4] Direct alcohol fuel cells (DAFCs) with aforementioned fuels have shown the capability to be alternative power sources with excellent efficiency and power generation ability.[5] For instance, methanol based fuel cells (DMFC) and ethanol based fuel cells (DEFC) have been studied in detail for some time now and many state of the art electrocatalysts have been reported in the literature.[6-8] While considering the performance capability of alcohol based DLFC systems, fuel cell systems based on alkaline medium have shown to be better compared to acidic systems. High OH^- ion concentration available in alkaline systems have shown to enhance fuel oxidation kinetics,[9-10] thus enabling superior performance. Among the different types of low molecular weight alcohols, Ethylene Glycol (EG) has gained much attention very recently, due to its properties like high boiling point (197.3 °C), low vapor pressure (8Pa at 20 °C) and also its lower toxicity. As it is known, during ethanol oxidation there is a difficuty in breaking the C-C bond at temperatures < 100 °C leading

Catalysis Science & Technology Accepted Manuscript

View Article Online
DOI: 10.1039/C8CY02232A

Published on 17 December 2018. Downloaded on 12/18/2018 12:59:19 AM.

formation of acetate and drop in faradic efficiency due to the imbalnce between the theoretical (12 electron per ethanol molecule) and actual (4 electron) electron transfer rate; ETR. This opens the way for an alternative fuel having high ETR and ethylene glycol is obviously an excellent choice owing to the high ETR of ~80% and formation of oxalate in alkaline medium. Furthermore, the electron transfer rate (ETR) during EGOR can be as high as 80%, indicating a higher Faradic efficiency compared to for e.g. ethanol (with ETR of 33%) during the alkaline direct oxidation. Ethylene glycol could be synthesized from biomass resources (for eg; cellulose) and other green synthesis techniques including electrochemical reduction of CO_2.[11-15] From the foregoing discussions, it is clear that EG is a highly potential candidate as fuel in liquid fueled energy carrier systems. However, one of the main limitations affecting the wide spread applicability of EG as fuel is the lack of high performance anode catalysts for its efficient electro oxidation.

The electro-oxidation of EG is a complex process, and the complete EG oxidation proceeds through a 10 e^-/molecule (Eq.1), resulting CO_2 as the product; [12]

$$HOCH_2 - CH_2OH + 10OH^- \rightarrow 2CO_2 + 8H_2O + 10e^- \quad E^0_a = -0.81V \ldots\ldots\ldots\ldots\ldots (1)$$

The above EG oxidation process proceeds through several intermediate steps giving rise to various intermediate products; the oxidation path and formation of intermediate products is reportedly dependent on the pH of the medium. An *in situ* FTIR study reported by Wang *et al* suggests that both, C_2 species (glycolate, glyoxalate and oxalate) and C_1 species (formate and carbonate) are formed in shared concentrations depending on the pH and on the other hand CO_2 is selectively produced in acidic solution.[16] Palladium has emerged as the most suitable candidate to replace Pt, while considering the alkaline anode oxidation of alcohol fuels. Pd-based catalysts have been comprehensively studied and analyzed recently for the effective oxidation of liquid

Catalysis Science & Technology Accepted Manuscript

View Article Online
DOI: 10.1039/C8CY02232A

Published on 17 December 2018. Downloaded on 12/18/2018 12:59:19 AM.

fuels.[17-22] However; it is a fact that efficient strategies need to be adopted to overcome the shortcomings associated with the use of Pd electrocatalysts in alkaline medium including durability, surface adsorption of poisoning intermediate species and enhancing the oxidation kinetics. Many techniques have been employed by researchers to improve the overall fuel oxidation kinetics of Pd; including bimetallic alloying, forming core-shell structures and doping with metal oxides.[23-28] Also, using supporting material including carbon for anchoring metal catalysts including Pd has further improved the activity of these catalysts by virtue of enhanced electroactive surface area, promoted electron–transfer and improved diffusion of electroactive species through the porous structure.[29] The addition/incorporation of metal oxides has previously shown to have enhanced the fuel oxidation kinetics of Pd, essentially from the increased OH^- concentration contributed by these oxides.[30-33] Amongst these oxides, $CeO_{2;}$ has been proven capable of various oxidation reactions due to its unique ability of oxygen storage. This property arises from the change in Ce oxidation states (Ce (IV) and Ce (III)), wherein the oxygen released during the Ce (IV) to Ce (III) reduction leading to formation of oxygen vacancies within the crystal structure.[33-35, 42] In previous studies involving Pd and Ce, Xu *et al* has demonstrated the slightly enhanced EOR capability for Pd/C with CeO_2 added, compared to commercial Pd/C in alkaline medium with a higher Pd–CeO_2 ratio (2:1 by weight) and higher Pd loading (0.3 mg cm^{-2}).[36] Palladium particles obtained via electroless technique was reduced on a carbon-ceria mixture obtained by Bambagioni *et al*, however with identical current density compared to Pd/C towards EOR in alkaline medium.[37] Palladium particles deposited on carbon- ceria conductive support was used by Miller *et al* to study hydrogen oxidation reaction in alkaline medium[38-39] and to test direct formate fuel cell performance.[40] However, to the best of our knowledge, a systematic study on the variation in electrooxidation performance of Pd in alkaline medium

Catalysis Science & Technology Accepted Manuscript

View Article Online
DOI: 10.1039/C8CY02232A

towards alcohol oxidation (EGOR MOR, EOR, etc.) with varying Pd - CeO_2 ratio and carbon-ceria ratios are not at all reported so far.

Herein, for the first time, we report a systematic assessment on the alkaline anodic oxidation competence of palladium nanocatalysts reduced over carbon-ceria composite support (Pd/C-CeO_2) for the low molecular weight alcohol fuel; ethylene glycol (EGOR). We have carefully analyzed the electro-oxidation kinetics of ethylene glycol with changing palladium – ceria interaction from the ceria infused carbon support. The altered carbon to ceria weight ratio in C-CeO_2 (1:0.5 to 1:2) composite enables the formation of various compositions of Pd/C-CeO_2 catalysts. The strategy adopted for the catalyst processing could be effectively scaled up for commercialization purposes. The prepared catalysts were also tested for alkaline oxidation of other liquid alcohol fuels including ethanol and methanol under identical conditions to testify the multi-fuel oxidation efficiency of the prepared catalysts. The role of CeO_2 in providing the excellent enhancement in electrocatalytic EGOR activity and stability of palladium is discussed on the basis of the electrochemical performance and catalyst characterizations.

Published on 17 December 2018. Downloaded on 12/18/2018 12:59:19 AM.

Catalysis Science & Technology Accepted Manuscript

View Article Online
DOI: 10.1039/C8CY02232A

Published on 17 December 2018. Downloaded on 12/18/2018 12:59:19 AM.

2. Experimental

The Pd nanoparticles were processed from K_2PdCl_4 (Furuya Chemicals, Japan) and the ceria-carbon composite support samples were prepared from $H_8N_8CeO_{18}$ (Ammonium Cerium (IV) Nitrate, TCI Chemicals, Japan) and Ketjen black (KB) (Lion Specialty Chemicals Co., Ltd., Japan) respectively. Triethylene glycol (TEG) used for Pd reduction was purchased from TCI Chemicals and PVP (K30) was supplied by Wako Chemicals, Japan. All chemicals (analytical grade) were used as received. Millipore water (Merck Millipore 3x Essential, Germany) having a resistivity of 18.2 MΩ/cm was used for the entire processing and other analysis.

2.1 Carbon-CeO_2 composite support synthesis

Varying compositions of carbon-ceria (1:0 - 1:2) support samples were prepared and used as support in this study for the reduction of Pd nanoparticles. In a typical synthesis of 1:1 wt% carbon –ceria composite support, 1 g KB carbon was initially (well) dispersed in 250 ml water by ultra-sonication (30 min). The ceria salt solution obtained by dissolving 3.183 g cerium ammonium nitrate (CAN), in 20 ml water was added drop-wise to this carbon slurry under stirring condition. Stirring was continued for additional 60 min after completion of the drop wise addition. 10 wt% solution of ammonia was then added drop wise under vigorous stirring until the pH reached 12. After stabilizing the pH, the mixture was ultra-sonicated for 30 min and then kept for overnight stirring. The mixture was centrifugally washed several times using millipore water and dried at 80 °C in a hot air oven. The dried composite precursor was heated to 200 °C in air atmosphere to obtain the C-CeO_2 composite support material.

Catalysis Science & Technology Accepted Manuscript

View Article Online
DOI: 10.1039/C8CY02232A

Published on 17 December 2018. Downloaded on 12/18/2018 12:59:19 AM.

2.2 Pd/C-CeO_2 catalyst processing

Palladium nanoparticles were synthesized over various compositions of the C-CeO_2 composite support materials, employing a polyol reduction,[41] (involving solid-solution processing) with modifications. In a typical synthesis, 0.326 g K_2PdCl_4 was initially dissolved in 15 ml millipore water. The Pd salt solution was further mixed with pre-prepared PVP solution (0.056 g PVP in 35 ml of water), followed by ultra-sonication for 30 min. After sonication, 0.2 g of C-CeO_2 composite powder was added to the above mixed solution and dispersed by sonication for 30 min. In the solid-solution processing of Pd nanoparticles, the aqueous Pd salt- C-CeO_2 mixture was sprayed to hot TEG solution (kept at 200 - 202 °C) under stirring. The Pd/C-CeO_2 powder material collected after centrifugal washing was dried overnight at 80 °C. A control sample of Pd/C catalyst was also processed under similar conditions for comparison of properties and performance.

2.3 Catalyst Characterization

The thermal decomposition characteristics of the as-prepared catalysts were analyzed under N_2 atmosphere at a heating rate of 2.5 °C/min using a Pyris 1 thermogravimetric analyzer (Perkin Elmer, USA). The phase analysis of the synthesized catalysts and catalyst support was analyzed using XRD patterns recorded at a scan rate of 1°/min using Ultima IV (Rigaku, Japan) system with a Cu Kα (λ = 1.5406 Å) x-ray source operating at 40 kV and 40 mA. HR-TEM micrographs were captured using a TOPCON EM-002BF-J system operating at an accelerating voltage of 200 kV with a twin EDS facility for insights on morphology and elemental distribution of the catalysts. An x-ray photoelectron spectrometer; Quantum 2000 (ULVAC-PHI Inc., Japan) fitted with a twin-anode x-ray source using Al Kα radiation (hv = 1486.58 eV) was used to analyze the surface

Catalysis Science & Technology Accepted Manuscript

View Article Online
DOI: 10.1039/C8CY02232A

composition of the catalysts. Gauss-Lorentz function of wave shape was used for fitting the curve and the background was revised using Shirley.

2.4 *Electrochemical Measurements*

HZ-7000 electrochemical measurement system and a dynamic electrode HR-301 (HD, Hokuto Denko) was used for electrochemical measurements of the prepared catalysts, including cyclic voltammetry (CV) and chronoamperometry (CA). CV evaluation of ethylene glycol oxidation (EGOR), ethanol oxidation (EOR) and methanol oxidation (MOR) performance were carried out using a three-electrode system with Hg/HgO and a Pt wire as the reference and counter electrodes, respectively. A glassy carbon electrode (GCE) with a surface area of 0.196 cm^2 was used as the working electrode and the current density observed was normalized with this surface area. The CV profiles were recorded in N_2-saturated 1 M KOH solution. To analyze the liquid fuel oxidation kinetics after CV cycle in 1M KOH solution; $(CH_2OH)_2$, CH_3CH_2OH, and CH_3OH were added in the range of 0.1 M – 1 M. For the catalyst ink preparation, catalyst ('y' mg) was mixed with 20 µL of Nafion (5 wt%) and 5 mL of IPA (25wt %), followed by ultrasonication in an ice bath for ~2 h. The glassy carbon electrode surface was modified by drop casting 10 µL of the catalyst ink, which was then dried overnight to form a film over the electrode surface. A uniform catalyst loading (15 $\mu g/cm^2$) on the GCE was maintained for all the catalyst compositions. The chronoamperograms were recorded at different corresponding potentials in N_2-saturated 1 M KOH + 1 M liquid fuel solutions.

Published on 17 December 2018. Downloaded on 12/18/2018 12:59:19 AM.
Catalysis Science & Technology Accepted Manuscript

View Article Online
DOI: 10.1039/C8CY02232A

Published on 17 December 2018. Downloaded on 12/18/2018 12:59:19 AM.

3. Results and Discussion

3.1 *Characterization of Catalysts*

The phase identification of the prepared catalysts and the support materials were carried out using X-ray diffraction experiments. Figure 1a shows the XRD patterns observed for C-CeO_2 (1:1) composite support, Pd/C, and Pd^{2+} reduced over C-CeO_2 (1:1). The Pd formation on C-CeO_2 is clearly indicated by the well-indexed peaks corresponding to Pd; peaks corresponding to CeO_2 could also be seen in the X-ray diffraction pattern. The peak signal at ~40° 2θ corresponds to the formation of *fcc* facets of metallic Pd particles along the 111 plane. The average crystallite size for Pd was calculated using Scherrer equation as ~ 6.3 nm. The thermal behavior of the Pd/C and Pd/ C-CeO_2 (1:1) catalyst in N_2 atmosphere is provided in Figure 1b. As shown, the total residual metal content increased from 36 wt % for Pd/C to 50 wt % for Pd/C-CeO_2 (1:1) indicating the presence of CeO_2 in the catalyst, which is in agreement with the X-ray diffraction data. The lowering of the decomposition temperature of carbon in the Pd/C-CeO_2 sample could be due to the oxidizing character of CeO_2.[42] The amount of Pd was found to be 27 wt% from ICP measurement and CeO_2 content was calculated as 23 wt%. The final Pd and CeO_2 content variation among the different catalyst compositions including Pd/C after thermal decomposition analysis are in the range of 20-36 wt% (*Table S1*).

Catalysis Science & Technology Accepted Manuscript

View Article Online
DOI: 10.1039/C8CY02232A

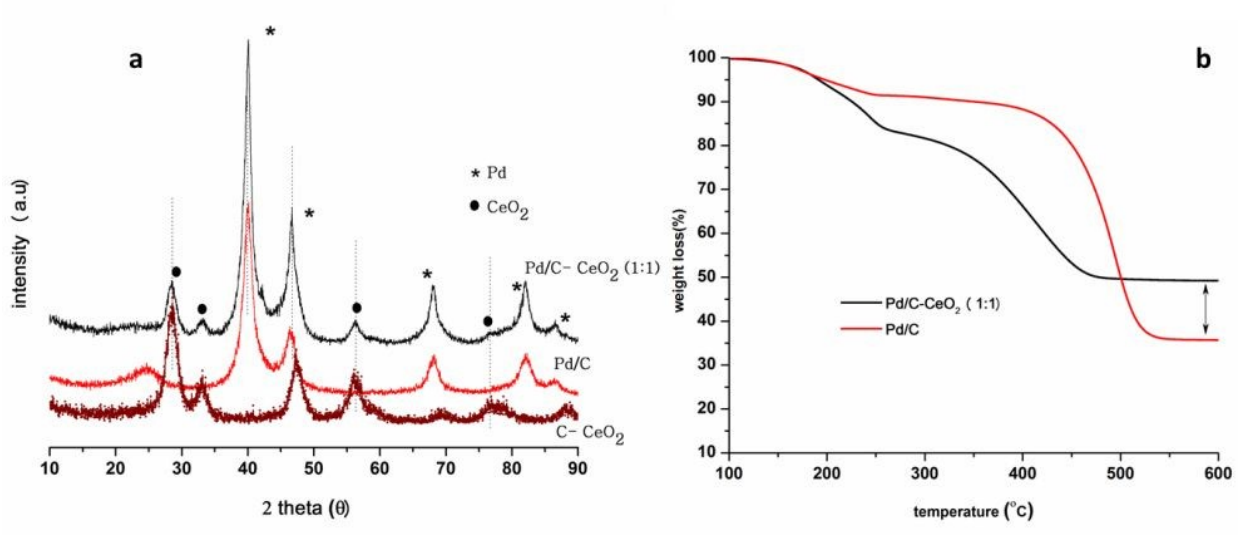

Figure 1. *(**a**) XRD patterns of C-CeO_2 (1:1), Pd/C and Pd/C-CeO_2 (1:1) catalysts (**b**) TGA patterns recorded for Pd/C and Pd/C-CeO_2 (1:1) catalysts*

The morphological evaluations of the carbon –ceria composite and Pd deposited catalysts were performed using transmission electron microscopy. Figure 2c shows the image of uniformly distributed spherical shaped palladium nanoparticles over the composite support. The corresponding EDS mapping and spectra recorded for the catalysts sample, as shown in (*Figure S1*), confirmed the successful reduction of the metal salt forming the uniform distribution of Pd over the carbon-ceria support. Figure 2d shows the lattice fringes corresponding to *fcc* facets of Pd (~ 0.23 nm) and cubic CeO_2 (0.32 nm). The average size of Pd nanoparticles was found to be ~6.5 nm in line with the XRD results. The size of Pd has increased slightly in the presence of CeO_2 compared to ~6 nm for Pd/C (*Figure S2*). It should be noted that the size of ceria also increased with increasing CeO_2 concentration in the support as depicted in Figure 2(a& b) (i.e., C- CeO_2 ratio from 1:1(~6 nm) to 1:2 (~15 nm)). The surface composition of the as prepared catalysts was analyzed using XPS and Figure 2(e) shows the deconvoluted spectra regions for Pd 3d and Ce 3d of Pd/C-CeO_2 (1:1). The XPS spectra once again confirmed the successful reduction of Pd metal salt over the composite support as evidenced by the peaks of Pd and CeO_2

Published on 17 December 2018. Downloaded on 12/18/2018 12:59:19 AM.
Catalysis Science & Technology Accepted Manuscript

View Article Online
DOI: 10.1039/C8CY02232A

(*Figure S4*). A slight positive shifting of the binding energy, by 0.25 eV for Pd 5/2 from 335.3 eV for Pd/C[43] to 335.55 eV for the Pd/C-CeO_2, was observed indicating a change in the electronic environment. It could also be seen that the Pd surface consists of peaks ascribed to metallic Pd (Pd 5/2, 335.55 eV) and PdO_2 (Pd 3/2), 341.1 eV).[43] With the well-known oxygen non-stoichiometric storage and mobility in CeO_2, oxidation of part of the Pd atoms close to CeO_2 surface is not surprising. In the Ce 3d region, the binding energy of 3d 5/2 was found at 883.07 eV for the Pd/C-CeO_2 compared to 83.03 eV in the C-CeO_2 support indicating an effective electronic interaction and charge transfer between Pd and CeO_2, which would turn out to be advantageous for fuel oxidation in alkaline medium.

Published on 17 December 2018. Downloaded on 12/18/2018 12:59:19 AM.

Catalysis Science & Technology Accepted Manuscript

View Article Online
DOI: 10.1039/C8CY02232A

Published on 17 December 2018. Downloaded on 12/18/2018 12:59:19 AM.

Catalysis Science & Technology Accepted Manuscript

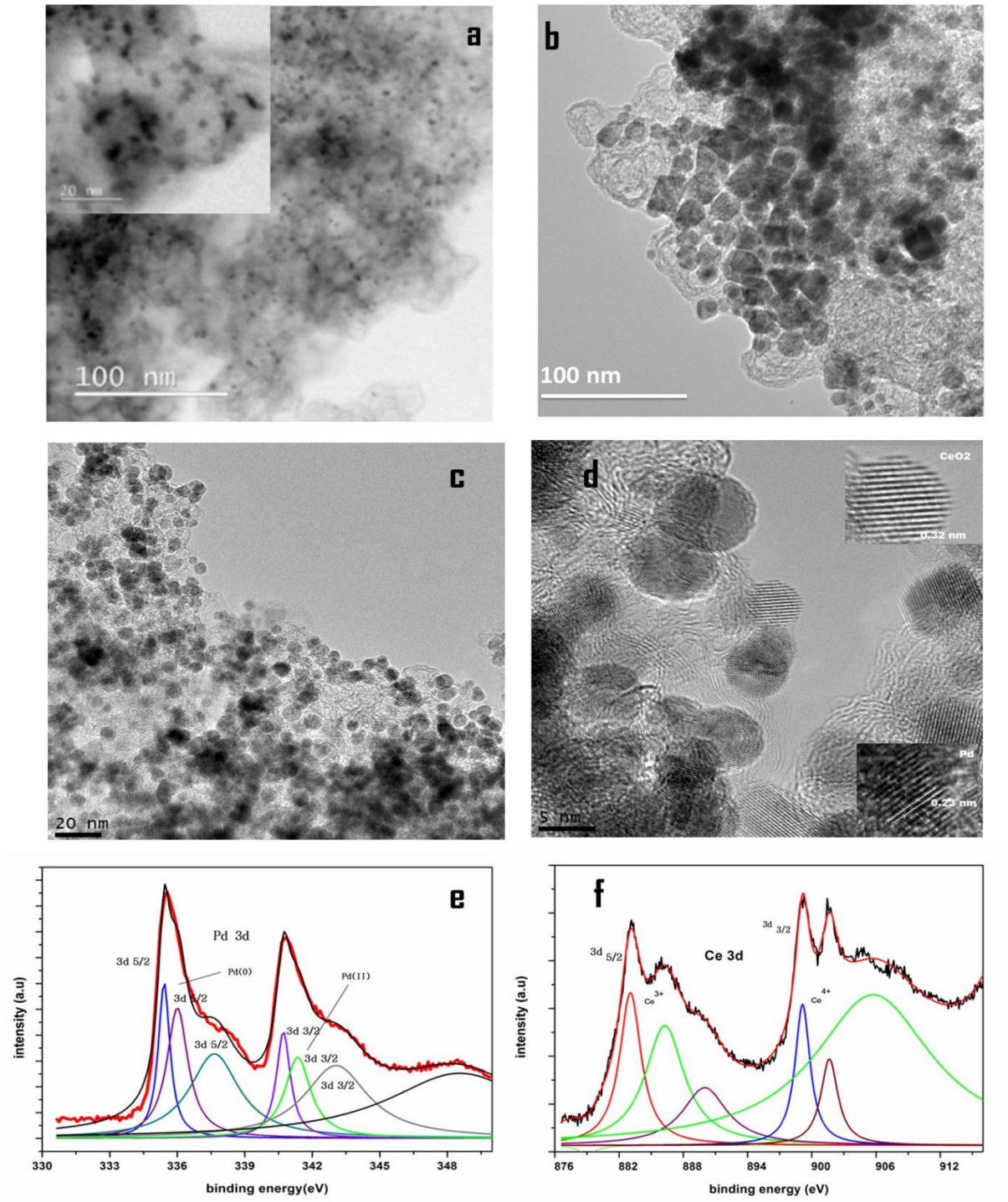

Figure 2. *HR-Transmission electron micrographs of* ***a)*** *C-CeO_2 (1:1) and b) C-CeO_2 (1:2) showing the agglomeration and size increase of ceria with increasing ratio/concentration* **c)** Low magnification *HR-TEM image of Pd/C-CeO_2 (1:1) showing the Pd distribution* **d)** *HR-TEM image of Pd/C-CeO_2 (1:1) showing the lattice fringes and size of Pd and CeO_2* **;** *XPS spectra and valence states with* **e)** *3d core regions of Pd and* **f)** *3d Ce after formation of Pd/C-CeO_2 (1:1) catalyst*

View Article Online
DOI: 10.1039/C8CY02232A

Published on 17 December 2018. Downloaded on 12/18/2018 12:59:19 AM.

3.2 *Electrochemical Characterization*

The cyclic voltammetry profiles obtained for the Pd/C and various Pd/C-CeO_2 catalyst samples in 1M KOH, measured in the range -0.9 – 0.2 V vs Hg/HgO at a scan rate of 50 mVs^{-1} are provided in Figure 3a. The recorded CVs showed typical characteristics of Pd based nano catalysts in alkaline medium.[43] The peak around –0.7 V in the forward (anodic) scan corresponds to the absorbed hydrogen and in the backward scan (cathodic) corresponds to hydrogen uptake. The current increase seen at around –1.0 V in the forward scan indicates the starting of Pd-O formation on the catalyst surface which is seen reduced in the reverse scan at ~ – 0.2 V vs Hg/HgO. The Pd-O peak observed for the ceria supported samples is seen to be enhanced compared to Pd/C catalyst sample. The Pd-O reduction peak intensity is observed to be high for Pd/C-CeO_2 (1:0.25), Pd/C-CeO_2 (1:0.5), *and* Pd/C-CeO_2 (1:1) compared to Pd/C while Pd/C-CeO_2 (1:1.5) which has increased ceria content showed only a very minimal Pd-O reduction peak. This change should be due to the large agglomeration of Pd nanoparticles formed (*Figure S3*) while reduction over the support hindering the removal Pd-O layer, formed which can in turn affect the catalytic property.[44] The electrochemical surface areas (ECSA) of the prepared catalysts were calculated integrating the area of the peak associated with Pd-O reduction (~ –0.2 V vs Hg/HgO) from the corresponding CV profiles. Although the particle size and morphology of Pd are similar in all the samples; as depicted in the recorded CV profiles, there is a certain change in the charge densities (Q) associated with Pd-O removal and Pd/C-CeO_2 (1:1) has the highest density among the measured samples leading to larger ECSA value. Figure 3b shows the variation in ECSA values for the different catalyst compositions, wherein Pd/C-CeO_2 (1:1) showing the maximum ECSA compared to that of Pd/C and other compositions. The ECSA of the Pd catalysts varied in the order; Pd/C-CeO_2 (1:1) > Pd/C-CeO_2 (1:0.5) > Pd/C > > Pd/C-CeO_2 (1:1.5) > Pd/C-CeO_2 (1:2).

Catalysis Science & Technology Accepted Manuscript

View Article Online
DOI: 10.1039/C8CY02232A

Published on 17 December 2018. Downloaded on 12/18/2018 12:59:19 AM.

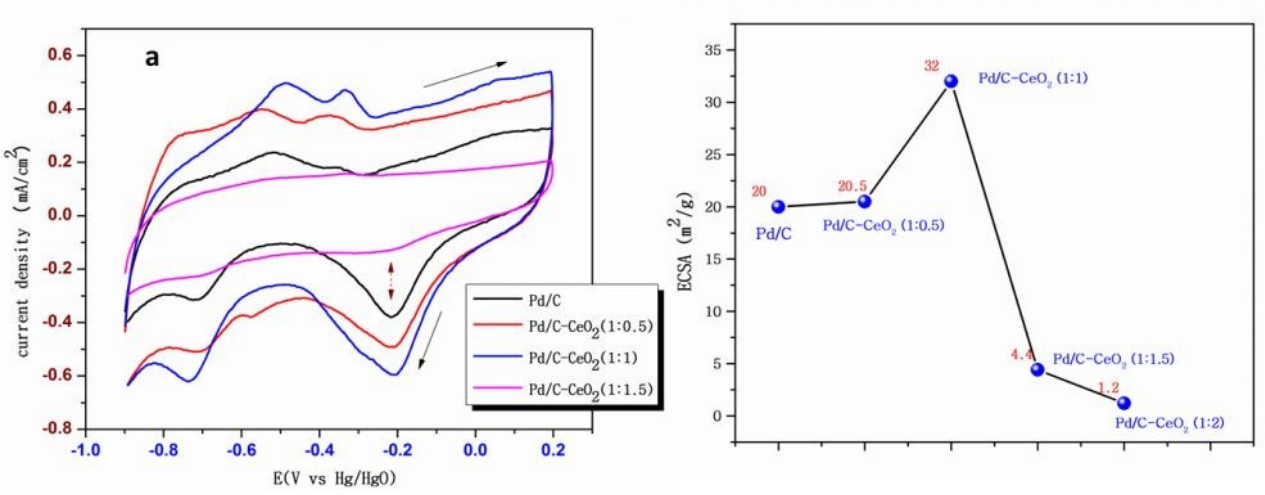

Figure 3a) *Cyclic voltammograms of Pd/C, Pd/C-CeO_2 (1:0.5), Pd/C-CeO_2 (1:1) and Pd/C-CeO_2 (1:1.5) catalysts in N_2-saturated 1 M KOH at 50 mV s^{-1}* ***b)*** *ECSA (m^2/g_{Pd}) variation among the as prepared catalysts calculated from Pd-O reduction peak*

2.3 Liquid Fuel Oxidation Kinetics

2.3.1 Ethylene Glycol Oxidation Reaction (EGOR)

During the ethyelene glycol oxidation in alkaline medium the consumption of OH^- occurs regardless of the substrate and during its oxidation in alkaline medium using Pd has resulted in glycooxalate formation and finally forming CO_2.[16] The CV forward scan profiles of the various catalyst samples obtained during the oxidation of 1M EG and 1M KOH mixture is provided in *Figure 4a*. For the catalyst sample (Pd) supported on a 1:1 composition of C-CeO_2 , showed more negative onset potential during the EGOR oxidation. A shift in the peak potential (E_p) towards positive side during the ethyelene glycol oxidation using Pd/C-CeO_2 designates the process is irreversible.[45] The performances of all the catalysts were evaluated in terms of E_{onset}, forward anodic peak current density, respective mass activity and specific activities. The maximum and enhanced peak current density value of **68.5 mA/cm²** was observed for Pd/C-CeO_2

Catalysis Science & Technology Accepted Manuscript

View Article Online
DOI: 10.1039/C8CY02232A

Published on 17 December 2018. Downloaded on 12/18/2018 12:59:19 AM.

(1:1) followed by Pd/C-CeO_2 (1:0.5) showing 46.2 mA/cm^2 current density. The current density value obtained for Pd/C-CeO_2 (1:1) is more than two times that recorded for Pd/C (28.5 mA/cm^2) catalyst. While considering the practical fuel-cell operation combined with oxygen reducing cathode, the current density at peak potential, (E_p) correspond to a lower voltage (ie ~ <0.2 V). This means that the overpotential for EGOR at this potential is too high. In this regard, the current densities observed at −0.3 V for the catalysts, a much lower overpotential than E_p is extremely relevant. The current denisties −0.3 V vs Hg/HgO was observed in the order; Pd/C-CeO_2 (1:1) > Pd/C-CeO_2 (1:0.5) > Pd/C > Pd/C-CeO_2 (1:2). The negative over-potential measured is among the lowest obtained for EGOR catalysts and hence is expected to give significant enhancement in fuel performance compared to numerous other reported systems.[46] Table 1 summarizes the complete CV data obtained during EGOR using different catalyst compsositions. The excellent enhancement in oxidation current density for Pd/C-CeO_2 (1:1) and Pd/C-CeO_2 (1:0.5) catalysts in alkaline medium is due promotion of the EGOR kinetics of Pd by the effective CeO_2 interaction as evidenced by the structural evaluation. Figure 4b shows the variation in onset potential for the Pd/C, Pd/C-CeO_2 (1:1) and Pd/C-CeO_2 (1:0.5) catalysts. Onset potential is identified at the potential at which the catalyst yielded current density of 1 mA cm^{-2}. It can be seen that there is a more negative shift of the onset potential for the Pd/C-CeO_2 (1:1) from the Pd/C onset potential. This negative shifting is indicative of the better EGOR activity for the CeO_2 promoted Pd catalysts compared to Pd/C.[47] The mass activity of the catalysts at the peak potential showed a significant increase for the Pd/C-CeO_2 (1:1) catalyst (4.6 A/mg $_{Pd}$), which is ~2.5 times higher than obtained for bare Pd/C (1.8 A/mg). This mass activity value is higher than for many of the EGOR catalysts reported recently in alkaline medium. The mass activity variation graph among the various catalysts including Pd/C is shown in figure 4c and follows the order Pd/C-CeO_2 (1:1) > Pd/C-CeO_2

Catalysis Science & Technology Accepted Manuscript

View Article Online
DOI: 10.1039/C8CY02232A

Published on 17 December 2018. Downloaded on 12/18/2018 12:59:19 AM.

(1:0.5) > Pd/C > Pd/C-CeO_2 (1:2). The forward and backward CV profiles during alkaline EGOR for Pd/C, Pd/C-CeO_2 (1:1) and Pd/C-CeO_2 (1:2) could be seen in figure S5 (a). The mechanism involved during alkaline ethylene glycol oxidation (EGOR) involves the following steps; [48]

$(CH_2\text{- }OH)_{2(ads)} \rightarrow CH_2OH\ (CHO)$ ------- (2)

$CH_2OH\ (CHO) \rightarrow CHO\ (COO^-)$ ------- (3)

$CHO\ (COO^-) \rightarrow (COO^-)_2$ ------- (4)

Table 1. *Cyclic voltammetry data obtained for the EGOR in 1M KOH using different catalyst compositions*

	Onset Potential (E_{onset}) (V)	**Current Density at -0.3 V vs Hg/HgO (mA/cm²)**	**Peak Current Density (at E_p) (mA/cm²)**	**Specific Activity vs Hg/HgO (mA/ cm²)**	**Mass Activity after CA at -0.2 V vs Hg/HgO (mA/mg_{Pd})**
Pd/C	-0.30	1.2	28.5	9	75
Pd/C-CeO_2 (1:0.5)	-0.35	1.8	46.2	14.8	105
Pd/C-CeO_2 (1:1)	**-0.37**	**3.1**	**68.5**	**14.5**	**135**
Pd/C-CeO_2 (1:2)	-0.25	0.7	13.9	2.3	19

The durability for the catalysts were analyzed using chronoamperometry in N_2 saturated alkaline solution with 1M $(CH_2OH)_2$. Figure 4d shows the chronoamperograms recorded for the Pd/C-CeO_2 and Pd/C catalysts. The mass current values obtained after the CA tests are provided in table 1. After 4000s of measurement at a potential of -0.2 V vs Hg/HgO, Pd/C-CeO_2 (1:1) showed a higher residual mass current value of 135 mA mg^{-1}_{Pd} compared to 75 mA mg^{-1}_{Pd} for Pd/C

Catalysis Science & Technology Accepted Manuscript

View Article Online
DOI: 10.1039/C8CY02232A

Published on 17 December 2018. Downloaded on 12/18/2018 12:59:19 AM.

indicating the better durability during EGOR. Further, stability test for Pd/C-CeO_2 (1:1) for EGOR was carried out using CV for 200 cycles; Figure S6. It could be seen that even after the test for more than 2 h; the catalyst showed a residual activity of greater than 87% and almost unchanged onset potential indicating good longer term efficiency. The CA tests also confirm that Pd/C-CeO_2 (1:1) maintained a higher EGOR activity compared to Pd/C and can contribute to antipoisoning capability during commercialization involving long term application. The enhanced antipoisoning should be due to the reduced adsorption of the intermediate species on the Pd surface facilitated by CeO_2 due to the increased OH_{ads}, wherein CeO_2 acts as the source of the oxygen containing species for reaction with the intermediate species.

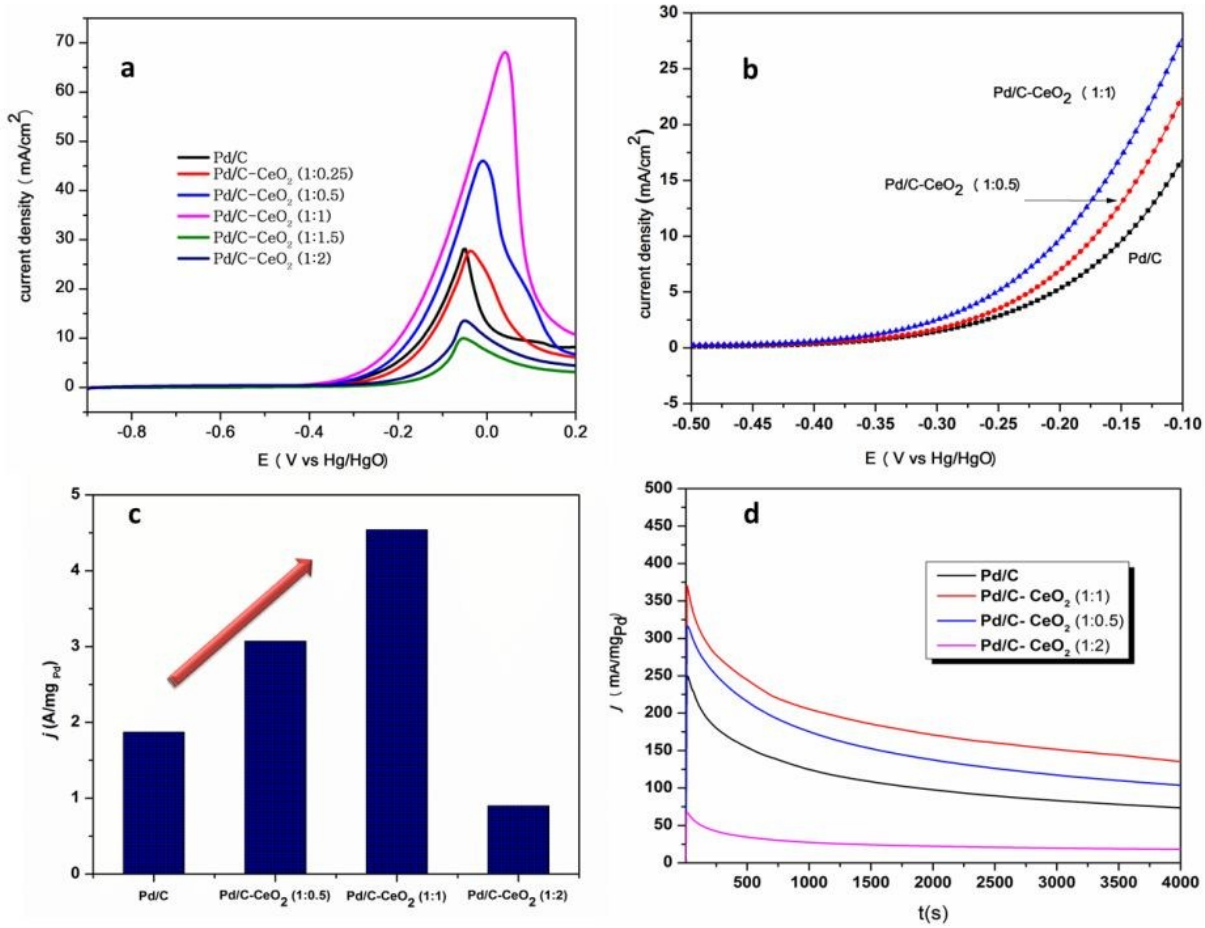

Figure 4. *Electrochemical data for the ethylene glycol oxidation reaction (EGOR) over Pd/C and Pd/C-CeO_2 (varying compositions)* ***a)*** *CVs with 1 M KOH + 1 M $(CH_2OH)_2$* ***b)*** *onset*

Catalysis Science & Technology Accepted Manuscript

View Article Online
DOI: 10.1039/C8CY02232A

*potential variation during forward scan obtained during EGOR (1M KOH + 1 M $(CH_2OH)_2$ **c)** mass activities of the catalyst samples at the peak potential **d)** chronoamperogram curves recorded for 4000s using catalyst casted GCE at -200 mV vs Hg/HgO in 1 M KOH*

The oxidation ability with increasing EG concentration for the Pd/C-CeO_2 (1:1) catalyst for alkaline EGOR is provided in *figure S5 (b)*. The possible creation and attachment of increased surface hydroxides on Pd surface by the optimum addition of CeO_2 has certainly helped in enhancing the oxidation kinetics of ethylene glycol in alkaline medium. The Pd/C-CeO_2 (1:1) catalyst composition prepared by the versatile solid-solution processing is thus demonstrated as the optimum catalyst composition for enhanced EGOR performance. The regeneration of active Pd sites by the strongly bound CeO_2/Pd has certainly improved the resistance towards poisoning species on the Pd surface.

2.3.2 Anodic oxidation of low molecular weight alcohols: Ethanol and Methanol

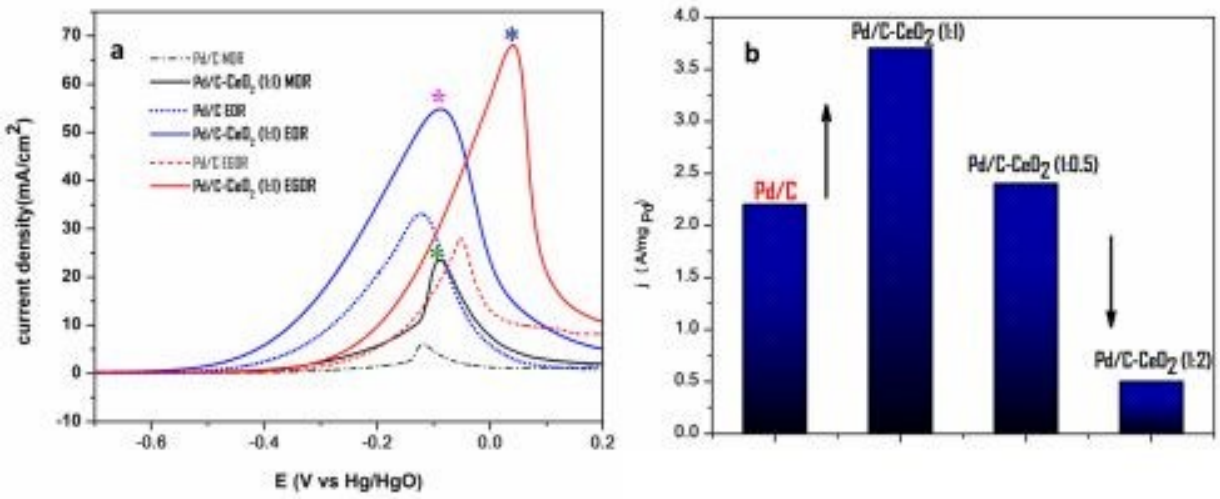

Figure 5. *Electrochemical data obtained for alkaline fuel oxidation for various fuels **a)** ethylene glycol oxidation reaction (EGOR), Ethanol oxidation reaction (EOR) and Methanol oxidation reaction (MOR) over Pd/C and Pd/C-CeO_2 (1:1) in 1 M KOH + 1 M Fuel **b)** mass activities observed for alkaline ethanol oxidation reaction (EOR) using Pd/C and Pd/C-CeO_2 catalysts*

Published on 17 December 2018. Downloaded on 12/18/2018 12:59:19 AM.
Catalysis Science & Technology Accepted Manuscript

View Article Online
DOI: 10.1039/C8CY02232A

Published on 17 December 2018. Downloaded on 12/18/2018 12:59:19 AM.

The electrochemical performance of the as prepared catalysts for the alkaline oxidation of other alcohol fuels; methanol and ethanol were also evaluated during our study. Figure 5 shows the comparison of the CV profiles observed during alkaline oxidation for methanol, ethanol and ethylene glycol fuels using the Pd/C-CeO_2 catalyst and Pd/C catalyst. It could be seen that Pd/C-CeO_2 (1:1) catalyst showed excellent enhancement in the oxidation kinetics than Pd/C for all the three fuels. The lower activity in the Pd/C-CeO_2 catalyst was observed during MOR which is in agreement with Matsuoka *et al* [49] and is due to the lower reactivity of methanol in alkaline direct alcohol fuel cell was when compared to that of ethylene glycol. The current density values obtained using Pd/C-CeO_2 catalyst varied in the order ethylene glycol > ethanol > methanol. The mass activities during the ethanol fuel oxidation reaction are depicted in figure 5b, normalized with the catalyst loading and the GCE surface area. Pd/C-CeO_2 (1:1) showed a mass activity value as high as 3700 mA/mg_{Pd} compared to 2400 mA/mg_{Pd} for Pd/C-CeO_2 (1:0.5) and 2200 mA/mg_{Pd} for Pd/C respectively. The increased tolerance to the poisoning species on the catalyst surface for the Pd/C-CeO_2 (1:1) and Pd/C-CeO_2 (1:0.5) evidenced by the higher mass activity values compared to Pd/C should be mainly due to the removal of intermediates from the surface by the OH_{ads}; facilitated by Pd-CeO_2 interaction.

The increased CeO_2 concentration has hindered the activity of Pd during alkaline oxidation of low molecular weight alcohols in Pd/C-CeO_2 (1:1.5) and Pd/C-CeO_2 (1:2) catalysts mostly due to the increased size of ceria and the large agglomeration of Pd particles leading to very less active catalytic sites. Therefore, the ideal Pd-CeO_2 interaction for efficient alcohol oxidation is possible only in the range of C-CeO_2 (1:1) and C-CeO_2 (1:0.5) concentrations.

4. CONCLUSIONS

Catalysis Science & Technology Accepted Manuscript

View Article Online
DOI: 10.1039/C8CY02232A

Published on 17 December 2018. Downloaded on 12/18/2018 12:59:19 AM.

For the first time, the effect of varying Pd- Ceria interaction and its effect towards alkaline EGOR performance was systematically analyzed and reported. Nano sized palladium catalysts were successfully obtained over varying weight percent ratios of carbon-ceria support (Pd/C-CeO_2), utilizing a versetalile solid-solution processing. The XPS and XRD data confirms the strong binding of Pd with the ceria infused composite support. The palladium catalysts; Pd/C-CeO_2 (1:1) and Pd/C-CeO_2 (1:0.5) showed enhanced oxidation kinetics towards ethylene glycol and better and enhanced stability in alkaline medium compared to Pd/C. The higher ECSA, more negative onset potential, high current density and excellent mass activity during anodic oxidation using Pd/C-CeO_2 (1:1) stamps the excellent effect of CeO_2 in optimal concentration for promoting the alkaline EGOR kinetics of Pd. With increasing CeO_2 content, the activity was found to be drastically reduced due to agglomeration of Pd particles leading large reduction in active catalytic sites. The enhanced formation of Pd-OH_{ads} favored by CeO_2 enabled the fast removal of poisoning species from the catalyst surface and enhanced the oxidation rate of alcohol as evidenced by electrochemical results. The enhanced durability of Pd/C-CeO_2 catalysts during EGOR compared to Pd/C has been confirmed by chronoamperometry and evidenced the strong Pd-CeO_2 interaction. Further, the EOR and MOR studies also depicted enhanced performance using the prepared Pd/C-CeO_2 catalysts. Results of the electrochemical catalyst property evidences the superiority of the catalysts prepared in our study along with identifying the factual Pd-Ce ratio for superior performance; and the simple yet scalable synthesis strategy adopted opens up the possibility for an time-bound commercialization of ceria promoted palladium nano catalysts as high efficient anode catalysts for applications in direct alcohol (alkaline) fuel cells (DAFCs).

Conflicts of interest

There are no conflicts to declare

Catalysis Science & Technology Accepted Manuscript

View Article Online
DOI: 10.1039/C8CY02232A

Published on 17 December 2018. Downloaded on 12/18/2018 12:59:19 AM.

Catalysis Science & Technology Accepted Manuscript

Acknowledgments

The authors acknowledge the financial assistance from the Japan Science and Technology (JST), Core Research for Evolutionary Science and Technology, Japan Science and Technology Agency (JST-CREST, JPMJCR1543). Mr. Masaaki Ito, R&D Center, Noritake Company Limited, Japan is kindly acknowledged for TEM and XPS analysis.

Electronic Supplementary Information (ESI) available: Additional TEM micrographs and EDS mapping of the composite support and the prepared catalysts, and the surface features (XPS) of the as prepared catalysts, cyclic stability of Pd- CeO_2 (1:1) catalysts and behavior of catalysts in varying alkaline concentration.

References

1. B.C. Ong, S.K. Kamarudin and S. Basri, International Journal of Hydrogen Energy, **2017**, 42, 10142

2. C. M. Miesse, W. S. Jung, K-J Jeong, J. K. Lee, J. Lee , J. Han , S. P. Yoon, S. W. Nam, T-H Lim and S-A Hong, J. power sources,**2006,** 162, 532

3. L. An, T.S. Zhao and Y.S. Li, Renew. Sustain. Energy Rev., **2015,** 50,1462 ; E. Antolini, J. power sources, **2007,** 170, 1

4. L. An and R. Chen, J. power sources, **2016**, 329, 484; H. Yue, Y. Zhao, X. Ma and J. Gong, Chem. Soc. Rev**.**, **2012,** 41,4218

5. E. Antolini, E. R. Gonzalez, Alkaline Direct Alcohol Fuel Cells, J. power sources 195 (**2010**) 3431–3450

View Article Online
DOI: 10.1039/C8CY02232A

Published on 17 December 2018. Downloaded on 12/18/2018 12:59:19 AM.

6. B. A. Kakade, T. Tamaki, H. Ohashi and T. Yamaguchi, J. Phys. Chem. C, **2012**, 116 (13), 7464

7. M.A.F. Akhairi and S.K. Kamarudin, International Journal of Hydrogen Energy,2016, 41, 4214

8. M.D. Obradovic, Z.M. Stanci, U.C. Lacnjevac , V.V. Radmilovic, A. Gavrilovic-Wohlmuther , V.R. Radmilovic and S. Lj. Gojkovic, Applied Catalysis B: Environmental, **2016,** 189, 110

9. S. Basri, S.K. Kamarudin, W.R.W. Daud and Z. Yaakub, International Journal of Hydrogen Energy, **2010,** 35, 7957

10. R. Dillon, S. Srinivasan, A.S. Arico and V. Antonucci, J. Power Sources, **2004,** 127, 112

11. T. Matsumoto, M. Sadakiyo, M. L. Ooi, S. Kitano, T. Yamamoto, S. Matsumura, K. Kato, T. Takeguchi and Miho Yamauchi, Sci. Rep., **2014**, 4, 5620

12. L. An and R. Chen, J. Power Sources, **2016,** 329, 484

13. M-Y. Zheng, A-Q. Wang, N. Ji, Ji-F. Pang, X-D. Wang and T. Zhang, ChemSusChem, **2010**, 3, 63

14. S. Ma , M. Sadakiyo , R. Luo , M. Heima , M. Yamauchi and P.J.A. Kenis, J. Power Sources, **2016**, 301, 219

15. D. Ren, Y. Deng, A. D. Handoko, C. S. Chen, S. Malkhandi and B. S. Yeo, ACS Catal., **2015, 5,** 2814

16. L. Wang, H. Meng, P. K. Shen, C. Bianchini, F. Vizza and Z. Wei, Phys. Chem. Chem. Phys., **2011,** 13, 2667

17. L. Zhang , Q. Chang , H. Chen and M. Shao, Nano Energy, **2016,** 29 198

18. Z.X. Liang, T.S. Zhao, J.B. Xu and L.D. Zhu, Electrochim. Acta, ,**2009,**54, 2203

19. C. Bianchini and P. K. Shen, Chem. Rev. **2009**, 109, 4183

20. W. Du, K.E. Mackenzie, D.F. Milano, N.A. Deskins, D. Su and X. Teng, ACS Catal., **2012,** 2 , 287–297

21. F. Yuan-Yuan, L. Zeng-Hua, Y. Xu, P. Wang, W. Wen-Hui and K. De-Sheng, J. Power Sources,**2013,** 232, 99

22. Y. Ma, T. Li, H. Chen, X. Chen, S. Deng, L. Xu, D. Sun and Y. Tang, J. Energy Chem., **2017,** 26, 1238

Catalysis Science & Technology Accepted Manuscript

View Article Online
DOI: 10.1039/C8CY02232A

Published on 17 December 2018. Downloaded on 12/18/2018 12:59:19 AM.

23. K. Mori, S. Masuda, H. Tanaka, K. Yoshizawa, M. Che and H. Yamashita, Chem. Commun., **2017,** 53,4677

24. X-Y. Ma, Y. Chen, H. Wang, Q-X. Li, W-F. Lin, W-B. Cai, Chem. Commun., **2018,** 54, 2562

25. S. Sankar, G. M. Anilkumar, T. Tamaki and T. Yamaguchi, ACS Appl. Energy Mater., **2018**, 1, 4140

26. J. Xue, G. Han, W. Ye, Y. Sang, H. Li, P. Guo and X. S. Zhao, ACS Appl. Mater. Interfaces, **2016,** 8, 34497

27. H. M. Song, D. H. Anjum, R. Sougrat, M. N. Hedhili, N. M. Khashab, J. Mater. Chem., **2012,** 22,25003

28. C. Wen, Y. Wei, D. Tang, B. Sa, T. Zhang and C. Chen, , Sci. Rep. ,**2017,** 7,4907

29. E. Antolini, Applied Catalysis B: Environmental, **2009,** 88, 1

30. Q. Liu, K. Jiang, J. Fan, Y. Lin, Y. Min, Q. Xu and W-B. Cai, Electrochimica Acta, **2016,** 203, 91

31. A. Dutta and J. Datta, J. Mater. Chem. A, **2014**, 2, 3237

32. H. Zhang, Y. Xie, Z. Sun, R. Tao, C. Huang, Y. Zhao, Z. Liu, Langmuir, **2011**, 27,1152

33. F. Carraro, A. Fapohunda, M. C. Paganini and S. Agnoli, ACS Appl. Nano Mater., **2018**, 1 1492

34. Q. He, S. Mukerjee, B. Shyam, D. Ramaker, S. Parres-Esclapez, M.J. Illan-Gomez and A. Bueno-Lopez, J. Power Sources, **2009,** 193, 408

35. Z.-K. Han, Y.-Z. Yang, B. B. Zhu, M. V. Ganduglia-Pirovano and Y. Gao, Phys. Rev. Materials, **2018,** 2, 035802-1

36. C. Xu, P. k. Shen and Y. Liu, J. Power Sources, **2007,** 164, 527

37. V. Bambagioni, C Bianchini, Y. Chen, J. Filippi, P. Fornasiero, M. Innocenti, Alessandro Lavacchi, A. Marchionni, W. Oberhauser and F. Vizza, ChemSusChem, **2012,** 5, 1266

38. H. A. Miller, A. Lavacchi, F. Vizza, M. Marelli,F. D. Benedetto, F. DAcapito, Y. Paska, M. Page and D. R. Dekel, Angew. Chem. Int. Ed., **2016,** 55, 6004

Catalysis Science & Technology Accepted Manuscript

View Article Online
DOI: 10.1039/C8CY02232A

39. H. A. Miller, F. Vizza, M. Marelli, A. Zadick, L. Dubau, M. Chatenet, S. Geiger, S. Cherevko, H. Doan, R. K. Pavlicek,, S. Mukerjee and D. R. Dekel, Nano Energy, **2017,** 33, 293

40. H. A. Miller, J. Ruggeri, A. Marchionni, M. Bellini, M. V. Pagliaro, C Bartoli, A Pucci , E. Passaglia and F. Vizza, Energies, **2018,** 11, 369

41. K. Sato, H. Tomonaga, T. Yamamoto, S. Matsumura, N.D.B. Zulkifli, T. Ishimoto, M. Koyama, K. Kusada, H. Kobayashi, H. Kitagawa and K. Nagaoka, Sci. Rep., **2016**, 6, 28265.

42. T. Montini, M. Melchionna, M. Monai and P. Fornasiero, Chem. Rev., **2016,** 116, 5987

43. M. Krawczyk and J.W. Sobczak, , Appl. Surf. Sci., **2004**, 235, 49

44. S. Mario, B. Steve, and C. Christophe, Appl. Catalysis B: Environ., **2010,** 93, 354

45. Q. He, S. Mukerjee, B. Shyam, D. Ramaker , S. Parres-Esclapez, M.J. Illan-Gomez and A. Bueno-Lopez, J. power sources, **2009,** 193, 408

46. D. R. Dekel, J. Power Sources, **2018**, 375, 158

47. H. Xu, P. Song, C. Fernandez, J. Wang, M. Zhu, Y. Shiraishi and Y. Du, ACS Appl. Mater. Interfaces , **2018,** 10, 12659

48. W Hong, C Shang, J Wang and E. Wang, Energy Environ. Sci., **2015,** 8, 2910

49. K. Matsuoka, Y. Iriyama, M. Matsuoka and Z. Ogumi, J. Power Sources ,**2005,** 150, 27

Published on 17 December 2018. Downloaded on 12/18/2018 12:59:19 AM.

Catalysis Science & Technology Accepted Manuscript

View Article Online
DOI: 10.1039/C8CY02232A

Electro-oxidation Competency of Palladium Nanocatalysts over Ceria-Carbon Composite Support during Alkaline Ethylene Glycol Oxidation

Sasidharan Sankar [†,‡], Naoto Watanabe [†], Gopinathan M. Anilkumar [§,‡], Balagopal N. Nair [§], Sailaja G. Sivakamiammal [±], Takanori Tamaki [†,‡], Takeo Yamaguchi [†,‡*]

[†] *Laboratory for Chemistry and Life Sciences, Tokyo Institute of Technology, R1-17, 4259 Nagatsuta, Midori-ku, Yokohama 226-850*
**E-mail: yamag@res.titech.ac.jp*

[‡] *Core Research for Evolutionary Science and Technology, Japan Science and Technology Agency (JST-CREST), Japan 102-0076*

[§] *R&D Centre, Noritake Co., Ltd., 300 Higashiyama, Miyochi-cho, Miyoshi, Japan 470-0293*

[±] *Cochin University of Science and Technology, Kochi, India 682022*

TOC

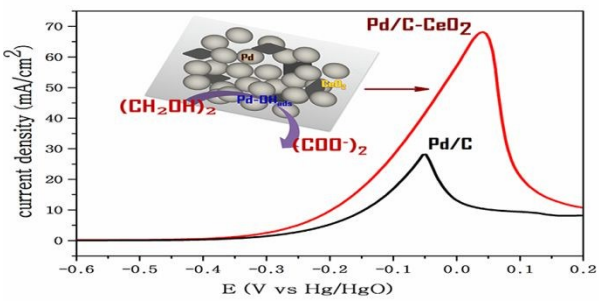

Effect of varying Pd-Ce interaction on the oxidation efficiency of ethylene glycol and low molecular weight alcohols in alkaline medium

Published on 17 December 2018. Downloaded on 12/18/2018 12:59:19 AM.

Catalysis Science & Technology Accepted Manuscript